# Assessment of mmWave Handset Arrays in the Presence of the User Body

C. Ballesteros, *Student Member, IEEE*, L. Vähä-Savo, K. Haneda, *Member, IEEE*, C. Icheln, J. Romeu, *Fellow, IEEE* and L. Jofre, *Fellow, IEEE*

***Abstract*—The emergence of mobile terminals operating at millimeter-wave (mmWave) frequencies necessitates the ability to evaluate the effect the environment and, in particular, users have on their radiation properties. Some studies evaluated the shadowing effects of a hand or an entire body for simple antenna configurations. This manuscript proposes a method for reliably predicting the performance of different array geometries in the presence of the users when they operate the mobile with one or with two hands. In practice, the way a mobile is operated is varying strongly between users and hence it is of great interest to draw a methodology to both numerically and experimentally evaluate any handset design in a large number of use cases in a repeatable manner. The use of numerical models and realistic phantoms allow high repeatability when evaluating the terminal radiation under real use conditions. Both the simulated body and the human phantom are used to study the field scattering from the handset arrays subject to the user interaction, yielding consistent results between them. Results suggest that shadowing by the user's torso usually decreases gain between 20–30 dB close to the region of the user. The user posture largely affects the spherical coverage, particularly for those antennas close to the corners in two-hand mode.**

***Index Terms*—5G handset, mmWave arrays, user modeling.**

## I. Introduction

THERE is a growing interest in studying the impact of the human body on the radiation of mobile terminals operating at frequency bands higher than the conventional sub-6 GHz. The body impact is particularly important when dealing with multiple-element antenna architectures and array geometries, which appear as the enabling technology for mmWave 5G communications [1] to overcome issues such as greater losses of diffraction around blocking objects as the frequency increases.

Over the last years, several numerical and experimental studies have been proposed. Wu, Rappaport and Collins lit the path in [2] with methods to evaluate the radiation in the presence of the human body and to evaluate the absorption of radiation. More recent works focused on the shadowing effect of the user and the coverage for phased antenna arrays on mobile phones [3]–[6]. These publications detail the performance degradation in terms of spherical coverage. They analyzed the radiation of one particular antenna array type and/or are limited to a single user position. Most results are from numerical simulations, while few experiments were carried out in presence of real users holding the phone with one hand. At a channel (far-field) level, the shadowing effect of the human body compared to a simplified geometric model is evaluated in [7] with a comprehensive study on the blockage loss. The evolution of the received power from a handset when it is held with one hand by a real user is also measured in [8]. The main drawback of previous studies is the lack of repeatability or generalization of the conclusions to other grip positions or antenna arrays, i.e., usage conditions. The 3rd Generation Partnership Project (3GPP) introduced in Rel-14 a model to cope with those issues related to repeatability and general applicability by proposing a 30 dB gain drop due to self-blockage, i.e., signal shadowing due to the user on its own handset. Nevertheless, other effects such as the reflection from the torso towards the back side of the phone (back radiation) are excluded [9].

In [10], a realistic phantom of a one-hand human body is proposed for the study of mmWave 5G terminals, where only the one-hand browsing mode is considered. The present work benefits from that methodology to provide a comprehensive study in the 28 GHz (n257 NR) band for two operation modes and three different array geometries both numerical and experimentally. Given the large bandwidth available in 5G FR2, which is mainly devoted to high-data-rate delivery to a mobile phone [11], only data browsing operation mode is considered from now on, thus no voice calls (phone close to the user's head) are assumed.

The main contributions of this work related to the aforesaid issues are therefore summarized as:

- Extend the proposed antenna evaluation methodology in [10] to more handset use cases and to different antenna arrays. Therefore, it is possible to find the most robust solution for relevant user postures according to location and inter-element distance of the antennas.
- Use of realistic human models in simulation and phantoms in measurements to provide a large degree of repeatability as in [10]. The impact of the user and antenna geometry is also compared to state-of-the-art findings.
- All situations are evaluated in terms of the figures of merit defined by the 3GPP standard [12] to be comparable to the industry requirements.

## II. Framework of the Study

In this section, the framework to study the interaction between the user and the mobile handset is described.

This work was supported by the Spanish Ministry of Economy under projects MDM2016-0600 and 2019-107885GB-C31 and the Ministry of Education with pre-doctoral grant FPU17/05561 to the first author. (*Corresponding author: Christian Ballesteros*)

C. Ballesteros, Prof. J. Romeu, and Prof. L. Jofre are members of the Antenna Laboratory (AntennaLab) at the UPC in Barcelona.

L. Vähä-Savo, K. Haneda, and C. Icheln are with the Department of Radio Science and Engineering from Aalto University, Espoo.

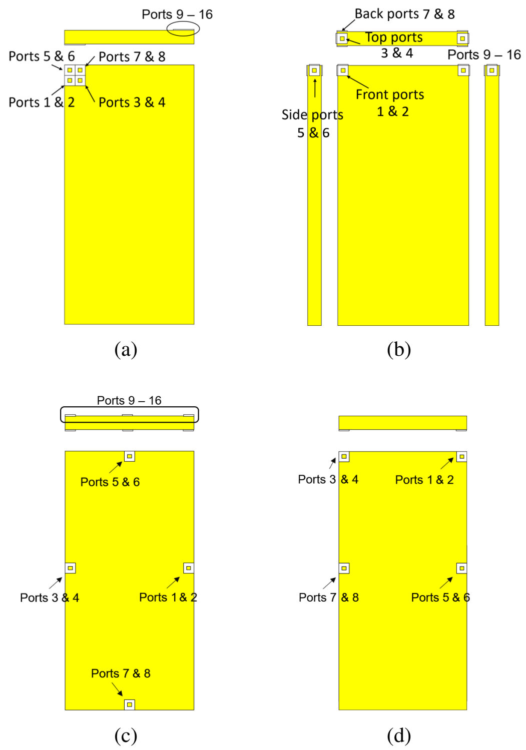


Fig. 1. UE handset array geometries. Arrays (a), (b) are used both in the simulated and experimental study, whereas (c) is only used in simulations (Section III) and (d), in the experimental campaign (Section IV). Ports 9–16 are pairwise equivalent to 1–8 on the second module.

### A. Handset mmWave Array Configurations

The antennas must be placed so that the radio link maintains its robust performance under the presence of a mobile user which affects antennas' radiation properties. Three antenna array configurations are considered, all composed of eight dual-polarised patch elements, as shown in Fig. 1 (from a to c). The first configuration is called co-located array (CA), already introduced in [10], consisting of two $2 \times 2$ patch arrays, one on the front and one on the back side, at the top corners of the phone. The second array is called as distributed array (DA), where four antenna elements are arranged around each top corners of the phone as a 3D array geometry. The edge array (EA) encompasses patch elements placed at the center of each edge of the phone, four per side. A metal cuboid, assumed as perfect electric conductor (PEC), with the dimensions 150 mm $\times$ 75 mm $\times$ 8 mm models the phone chassis.

### B. User Body Modeling

The methodology used to numerically model the human body of a user is detailed in [13]. The scattering of the body is computed by means the surface integral method. As a source, the near-field radiated fields of the handset array in presence of the hands are used, which are computed by means of finite-difference time-domain (FDTD) and a complete 3D mesh of the hands. The skin properties defined by [2] are sufficient to model the scattering of the human body, $\varepsilon_r$=16.55 and $\sigma$=25.82 S/m, since the penetration depth at 28 GHz is only about 1 mm [14], [15].

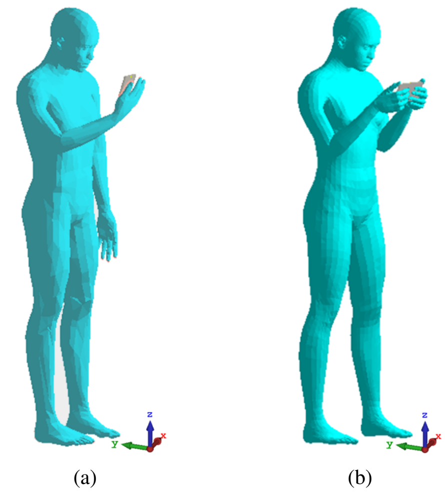


Fig. 2. Human postures modeling a realistic handset usage. (a) One-hand mode. (b) Two-hand mode.

TABLE I
TRANSMITTER AND RECEIVER SPECIFICATIONS FOR POWER CLASS 3 UE IN THE N257 NR BAND.

| **Min peak EIRP** | **Max EIRP** | **Min EIRP at 50%-tile CDF** |
|---|---|---|
| 22.4 dBm | 43 dBm | 11.5 dBm |
| **REFSENS**[1] | **EIS at 50%-tile CCDF** | |
| −88.3 dBm | −77.4 dBm | |

The user holds the phone with one or two hands, in front of his or her face, in browsing (multimedia) mode. Thus two operation modes are assumed, with one- or two-hand grip (see Fig. 2). The phone is tilted 20° away from the zenith direction in both cases.

### C. Performance Evaluation

Beam scanning is for the three arrays performed with one 3-bit phase shifter per port in computer simulations, and in each direction the maximum gain of the available 1024 beams is determined to analyze spherical coverage statistics.

Spherical coverage is usually analysed by means of the cumulative distribution function (CDF) of the effective isotropic radiated power (EIRP) (in transmission mode) or the effective isotropic sensitivity (EIS) (in reception) across different pointing angles. The 3GPP specifies the over-the-air (OTA) radio characteristics that the user equipment (UE) must satisfy in free space [12]. It is found relevant to investigate the degradation in those figures when the user is present. The requirements for power class 3, corresponding to mobile handsets, are detailed in Table I. The impact is equivalent in downlink or uplink and hence we analyse only the EIRP of the handset.

## III. NUMERICAL RESULTS

The three handset array configurations are studied in two operation modes, i.e., one- and two-hand grip in terms of their

[1]Values for 50 MHz bandwidth, 3 dB must be successively added for 100/200/400 MHz.

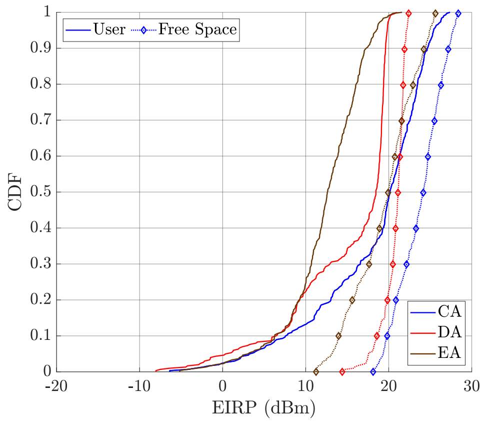


Fig. 3. Comparison of the EIRP CDF for the three arrays in one-hand mode.

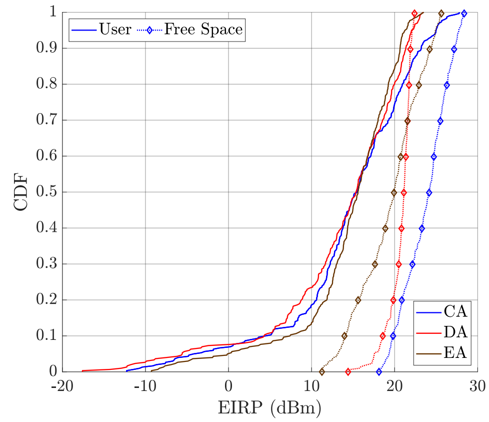


Fig. 4. Comparison of the EIRP CDF for the three arrays in two-hand mode.

TABLE II
VARIATION OF THE EIRP DUE TO A HUMAN BODY FOR THE THREE ARRAY GEOMETRIES UNDER ONE-HAND OPERATION.

| | CA | DA | EA |
|---|---|---|---|
| **△ peak EIRP (dB)** | −1.0 | −1.4 | −4.1 |
| **△ 50%-tile EIRP (dB)** | −4.0 | −2.7 | −7.3 |

TABLE III
VARIATION OF THE EIRP DUE TO A HUMAN BODY FOR THE THREE ARRAY GEOMETRIES UNDER TWO-HAND OPERATION.

| | CA | DA | EA |
|---|---|---|---|
| **△ peak EIRP (dB)** | −0.6 | 1.1 | −2.2 |
| **△ 50%-tile EIRP (dB)** | −8.7 | −5.8 | −4.4 |

EIRP. The transmit power is set to 10 dBm so the minimum peak EIRP of the three arrays in free space conditions fulfills the requirements from the 3GPP standard (Table I).

### A. One-hand Operation

The user's palm mainly affects the antennas mounted on the back side of a mobile phone case in one-hand data mode. Also the effect of the torso is significant, mainly on the front far-field radiation. Fig. 3 shows the CDF of the EIRP for the one-hand operation mode compared to the free-space case. The signal from the dual-polarized antennas is coherently combined. For all three array configurations, there is a clear degradation on the realized EIRP.

This degradation is summarized in Table II with the variation of the peak and median EIRP with respect to the free space. Negative values mean a degradation of the EIRP with the human body and positive values imply an improvement compared to the free-space radiation. The most affected geometry is the EA, in which back antennas are partially covered by the hand palm. The top corner arrays like CA and DA are able to radiate across the head and the self-blockage effect is somehow mitigated.

### B. Two-hand Operation

The same analysis is carried out for the two-hand mode. The phone structure is now rotated by 90° in a plane parallel to the screen. The palm covers the antennas on the short edges and corners, which is even translated in a slight detuning of the resonant frequency, also considered in the simulation. Fig. 4 represents the CDF of the EIRP in two-hand mode for the three aforementioned array configurations. The results show a noticeable loss with respect to free-space radiation and the tendency is similar for all arrays. Only the CA has a clear higher peak gain when the phone is held with two hands.

Table III details the loss in the spherical coverage for each case. The overall coverage is degraded due to the fact that both hands cover the phone and all antennas are right in front of the torso. Nevertheless, the peak gain is not that much affected compared to the one-hand operation. This is mainly due to the back radiation that reinforces those angles opposite to the user. Despite the larger degradation of the CA coverage, this geometry still appears to be the one reaching larger gain values both for one- and two-hand operation modes. However, in two-hand mode, the gain up to the 70%-tile for all geometries is practically the same.

## IV. EXPERIMENTAL VALIDATION

The performance of the handset antennas in presence of the user is now assessed through measurements in order to validate the numerical approach. Two human phantoms are built as in Fig. 5 to mimic the scattering effect of the human body when the user holds the mobile with one hand or with two hands, similarly to the two posture models in Fig. 2. The human phantom with one hand is used to measure the CA and DA configurations, where all the antennas are on the top corners of the phone. A prototype of mixed array (in Fig. 1d) with both edge and corner antennas is used with the two-hand phantom. The two types of antenna configurations are compared to provide further understanding of the actual effect of the hands close to the short edges. The EA design is not considered in this section. These results extend the methodology in [10] to two grip modes and three different handset arrays. The phantom does not include the effect of the lower legs, and polar angles greater than 150° are removed because of the shadowing of the mast holding the phantom in

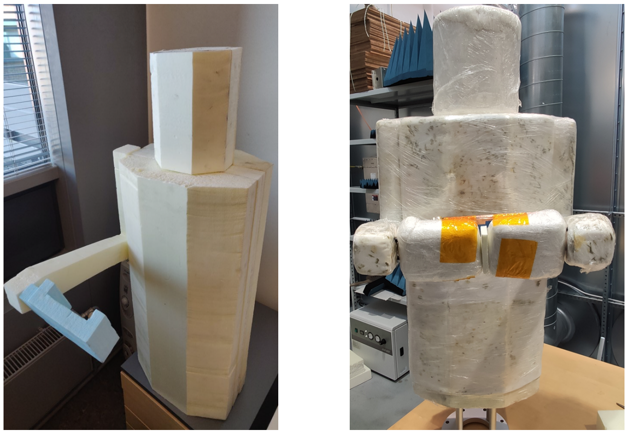

(a) (b)

Fig. 5. Human phantoms representing a mobile user. (a) One-hand phantom polystyrene body foundation before coating with skin material. (b) Two-hand phantom once covered with skin material.

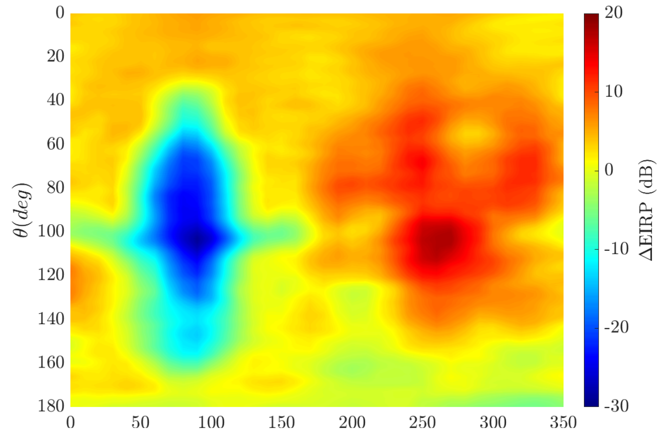


Fig. 6. Difference of EIRP between measured free-space and two-hand human phantom for the mixed array.

TABLE IV
DIFFERENCE OF THE HANDSETS' EIRP BETWEEN MEASUREMENTS AND SIMULATIONS OF USER'S POSTURES REPRESENTED IN FIG. 5 AND FIG. 2, RESPECTIVELY

| | **One hand** | | **Two hands** |
|---|---|---|---|
| | **CA** | **DA** | **Mixed Array** |
| **△ peak EIRP (dB)** | −0.1 | 4.9 | −0.6 |
| **△ 50%-tile EIRP (dB)** | −0.1 | −1.3 | 1.3 |

TABLE V
STATISTICS OF THE MEASURED HUMAN BODY SHADOWING (LOSS IN EIRP) COMPARED TO FREE-SPACE RADIATION. AS A REFERENCE, THE PARAMETERS OF BLOCKAGE MODEL A FROM THE 3GPP ARE SHOWN [9].

| | **One hand** | | **Two hands** | **3GPP TR 38.901** | |
|---|---|---|---|---|---|
| | **CA** | **DA** | **MA** | **Portrait** | **Landscape** |
| **Min ΔEIRP (dB)** | −29.1 | −28.3 | −28.2 | −30 | −30 |
| $\mathbf{x_{sb}}$ (°) | 40 | 60 | 50 | 120 | 160 |
| $\mathbf{y_{sb}}$ (°) | 99 | 97 | 57 | 80 | 75 |

the chamber. The measurements are performed with 1° and 10° resolution in polar and azimuth angles, respectively.

The far-field radiation of the measured arrays with the two phantom models is compared to the numerical results in terms of the EIRP CDF. Table IV depicts the difference between measured and simulated EIRP and the three aforementioned geometries. The results agree with small variance. The largest difference is for the DA, in which assembly inaccuracies and surface currents on the metal cuboid representing the phone chassis affect the actual performance of the prototype.

For illustration, Fig. 6 shows the EIRP difference between free-space radiation and the coverage in presence of the human phantom for the mixed array geometry in two-hand mode. As expected, the user shadows the region in front of the phone whereas some back radiation is reinforced, reaching higher values than those in free-space (particularly high for the CA and mixed arrays).

The spherical coverage is then compared to the simplified model of the 3GPP [9], which specifies the additional loss to those propagation paths within the self-blocking region. These results are also in line with those found in the literature as in [3], [13]. The effect of the body shadowing is then summarized in Table V in terms of the shadowing depth and its extent along the azimuth ($x_{sb}$) and elevation ($y_{sb}$) dimensions. The maximum additional loss agrees with the models of the 3GPP, while the 0-dB gain to other directions than the self-blocking region would not be true because of the existence of the back-radiation. In addition, the azimuth and elevation spans do not completely agree. In the experimental results, those are calculated by assuming self-blockage when losses are greater than 20 dB within the shadowed region as previously stated.

## V. Conclusion

This paper proposes a method to assess the performance of mmWave handset-antenna designs in the presence of a human user. The shadowing and scattering properties of the body are compared for two operation modes, holding the handset with one or with two hands. The study presents the achievable coverage of representative array geometries. A good agreement in the antenna radiation characteristics is found in terms of the CDF of the EIRP under the presence of a human body, both simulated and measured with a phantom.

It is demonstrated a high dependence between the array geometry, the operation mode and the self-blockage shadowing effect. The effect of the human phantom is compared to those blockage models defined by the 3GPP with small discrepancies. None of the arrays is found most robust for both one- and two-hand scenarios in terms of coverage. More dual-polarized antennas could be beneficial in this sense.

## References

[1] W. Hong, K. Baek, Y. Lee, Y. Kim, and S. Ko, "Study and prototyping of practically large-scale mmWave antenna systems for 5G cellular devices," *IEEE Communications Magazine*, vol. 52, no. 9, pp. 63–69, 2014.

[2] T. Wu, T. S. Rappaport, and C. M. Collins, "The human body and millimeter-wave wireless communication systems: Interactions and implications," in *2015 IEEE International Conference on Communications (ICC)*, June 2015, pp. 2423–2429.

[3] K. Zhao, J. Helander, D. Sjöberg, S. He, T. Bolin, and Z. Ying, "User Body Effect on Phased Array in User Equipment for the 5G mmWave Communication System," *IEEE Antennas and Wireless Propagation Letters*, vol. 16, pp. 864–867, 2017.

[4] I. Syrytsin, S. Zhang, and G. F. Pedersen, "User Impact on Phased and Switch Diversity Arrays in 5G Mobile Terminals," *IEEE Access*, vol. 6, pp. 1616–1623, 2018.

[5] R. Rodríguez-Cano, S. Zhang, K. Zhao, and G. F. Pedersen, "User Body Interaction of 5G Switchable Antenna System for Mobile Terminals at 28 GHz," in *2019 13th European Conference on Antennas and Propagation (EuCAP)*, March 2019, pp. 1–4.

[6] S. Zhang, X. Chen, I. Syrytsin, and G. F. Pedersen, "A Planar Switchable 3-D-Coverage Phased Array Antenna and Its User Effects for 28-GHz Mobile Terminal Applications," *IEEE Transactions on Antennas and Propagation*, vol. 65, no. 12, pp. 6413–6421, Dec 2017.

[7] U. T. Virk and K. Haneda, "Modeling Human Blockage at 5G Millimeter-Wave Frequencies," *IEEE Transactions on Antennas and Propagation*, vol. 68, no. 3, pp. 2256–2266, 2020.

[8] J. Hejselbæk, J. Ø. Nielsen, W. Fan, and G. F. Pedersen, "Measured 21.5 GHz Indoor Channels With User-Held Handset Antenna Array," *IEEE Transactions on Antennas and Propagation*, vol. 65, no. 12, pp. 6574–6583, Dec 2017.

[9] 3GPP, "Study on channel model for frequencies from 0.5 to 100 GHz (release 16)," TR 38.901 (V16.1.0), Dec. 2019.

[10] L. Vähä-Savo, C. Cziezerski, M. Heino, K. Haneda, C. Icheln, A. Hazmi, and R. Tian, "Empirical Evaluation of a 28 GHz Antenna Array on a 5G Mobile Phone Using a Body Phantom," *IEEE Transactions on Antennas and Propagation*, pp. 1–1, 2021.

[11] A. Narayanan, E. Ramadan, J. Carpenter, Q. Liu, Y. Liu, F. Qian, and Z.-L. Zhang, "A first look at commercial 5G performance on smartphones," in *Proceedings of The Web Conference 2020*, 2020, pp. 894–905.

[12] 3GPP, "User Equipment (UE) radio transmission and reception; Part 2: Range 2 Standalone (Release 16)," 3rd Generation Partnership Project (3GPP), Technical Specification (TS) 38.101-2, Jun 2019.

[13] M. Heino, C. Icheln, and K. Haneda, "Self-user shadowing effects of millimeter-wave mobile phone antennas in a browsing mode," in *2019 13th European Conference on Antennas and Propagation (EuCAP)*, March 2019, pp. 1–5.

[14] O. P. Gandhi and A. Riazi, "Absorption of Millimeter Waves by Human Beings and its Biological Implications," *IEEE Transactions on Microwave Theory and Techniques*, vol. 34, no. 2, pp. 228–235, Feb 1986.

[15] P.A. Hasgall, F. Di Gennaro, C. Baumgartner, E. Neufeld, B. Lloyd, M.C. Gosselin, D. Payne, A. Klingenböck, and N. Kuster, "IT'IS Database for thermal and electromagnetic parameters of biological tissues," May 2018, version 4.0.